

## RESEARCH ARTICLE

# Benzolamide perpetuates acidic conditions during reperfusion and reduces myocardial ischemia-reperfusion injury

Alejandro Ciocchi Pardo,<sup>1</sup> Romina G. Díaz,<sup>1</sup> Luisa F. González Arbeláez,<sup>1</sup> Néstor G. Pérez,<sup>1</sup> Erik R. Swenson,<sup>2</sup> Susana M. Mosca,<sup>1</sup> and Bernardo V. Alvarez<sup>1</sup>

<sup>1</sup>Centro de Investigaciones Cardiovasculares CIC-CONICET, Facultad de Ciencias Médicas, Universidad Nacional de La Plata, La Plata, Argentina; and <sup>2</sup>Division of Pulmonary and Critical Care Medicine, Department of Medicine, University of Washington, Department of Veterans Affairs Puget Sound Health Care System, Seattle, Washington

Submitted 20 October 2017; accepted in final form 18 December 2017

**Ciocchi Pardo A, Díaz RG, González Arbeláez LF, Pérez NG, Swenson ER, Mosca SM, Alvarez BV.** Benzolamide perpetuates acidic conditions during reperfusion and reduces myocardial ischemia-reperfusion injury. *J Appl Physiol* 125: 340–352, 2018. First published December 21, 2017; doi:10.1152/jappphysiol.00957.2017.—During ischemia, increased anaerobic glycolysis results in intracellular acidosis. Activation of alkalinizing transport mechanisms associated with carbonic anhydrases (CAs) leads to myocardial intracellular  $\text{Ca}^{2+}$  increase. We characterize the effects of inhibition of CA with benzolamide (BZ) during cardiac ischemia-reperfusion (I/R). Langendorff-perfused isolated rat hearts were subjected to 30 min of global ischemia and 60 min of reperfusion. Other hearts were treated with BZ (5  $\mu\text{M}$ ) during the initial 10 min of reperfusion or perfused with acid solution (AR, pH 6.4) during the first 3 min of reperfusion. p38MAPK, a kinase linked to membrane transporters and involved in cardioprotection, was examined in hearts treated with BZ in presence of the p38MAPK inhibitor SB202190 (10  $\mu\text{M}$ ). Infarct size (IZ) and myocardial function were assessed, and phosphorylated forms of p38MAPK, Akt, and PKC $\epsilon$  were evaluated by immunoblotting. We determined the rate of intracellular pH ( $\text{pH}_i$ ) normalization after transient acid loading in the absence and presence of BZ or BZ + SB202190 in heart papillary muscles (HPMs). Mitochondrial membrane potential ( $\Delta\Psi_m$ ),  $\text{Ca}^{2+}$  retention capacity and  $\text{Ca}^{2+}$ -mediated swelling after I/R were also measured. BZ, similarly to AR, reduced IZ, improved postischemic recovery of myocardial contractility, increased phosphorylation of Akt, PKC $\epsilon$ , and p38MAPK, and normalized  $\Delta\Psi_m$  and  $\text{Ca}^{2+}$  homeostasis, effects abolished after p38MAPK inhibition. In HPMs, BZ slowed  $\text{pH}_i$  recovery, an effect that was restored after p38MAPK inhibition. We conclude that prolongation of acidic conditions during reperfusion by BZ could be responsible for the cardioprotective benefits of reduced infarction and better myocontractile function, through p38MAPK-dependent pathways.

**NEW & NOTEWORTHY** Carbonic anhydrase inhibition by benzolamide (BZ) maintains acidity, decreases infarct size, and improves postischemic myocardial dysfunction in ischemia-reperfusion (I/R) hearts. Protection afforded by BZ mimicked the beneficial effects elicited by an acidic solution (AR). Increased phosphorylation of p38MAPK occurs in I/R hearts reperfused with BZ or with AR. Mitochondria from I/R hearts possess abnormal  $\text{Ca}^{2+}$  handling and a more depolarized membrane potential compared with control hearts, and these changes were restored by treatment with BZ or AR.

Address for reprint requests and other correspondence: B. V. Alvarez, Centro de Investigaciones Cardiovasculares CIC-CONICET, Facultad de Ciencias Médicas, Universidad Nacional de La Plata, Calle 60 y 120, 1900 La Plata, Argentina (e-mail: balvarez@med.unlp.edu.ar).

acidic reperfusion; benzolamide; carbonic anhydrase; mitochondria; myocardial infarction

## INTRODUCTION

The acute coronary syndrome resulting in myocardial ischemia and infarction is a major cause of morbidity and mortality worldwide. With myocardial infarction, early reperfusion is important in preserving as much myocardium as possible. However, injury initiated during reperfusion accounts for a sizable portion of cardiomyocyte damage, arrhythmias, and death following myocardial ischemia (45). Thus any strategies to limit the injurious effects of reperfusion may reduce both the mortality and the long-term morbidity of myocardial infarction.

Cardiac pH homeostasis is severely disturbed by ischemia. Intracellular pH ( $\text{pH}_i$ ) can decline by  $\sim 0.5$  pH units in  $<5$  min, with extracellular pH reaching values ranging from 6 to 6.5 during the ischemic stress (44). Reduced  $\text{pH}_i$  is protective to the heart via different mechanisms including inhibition of, e.g., mitochondrial permeability transition pore (MPTP) formation, gap junction conductivity, intracellular uptake of  $\text{Ca}^{2+}$  by membrane  $\text{Ca}^{2+}$  channels and  $\text{Na}^+/\text{Ca}^{2+}$  exchange, and activity of deleterious calpain and caspases among other cardiac cell death-trigger factors (26). Upon reperfusion, cardiac  $\text{pH}_i$  is rapidly restored by washout of  $\text{H}^+$  and activation of acid-extruding and base-uptake transport proteins, which allow opening of the MPTP leading to  $\text{Na}^+$  and  $\text{Ca}^{2+}$  overload, hypercontracture, necrosis, and apoptosis (40). Conversely, delayed  $\text{pH}_i$  recovery in isolated rat heart exerts a protective effect after global ischemia (25). This protection of reperfused ischemic tissues by acidic reperfusion has been observed in the heart and other organ ischemia-reperfusion (I/R) injuries (liver, brain, lung, kidney, and gastrointestinal tract) and has been termed the pH paradox (28, 33).

The two major ion transporters that contribute to normalization of  $\text{pH}_i$  in the heart after an acid load are  $\text{Na}^+/\text{H}^+$  exchanger (NHE)1 and the  $\text{Na}^+-\text{HCO}_3^-$  (NBC) cotransporters (58). Inhibition of NHE1 has been shown to exert protective effects in a large number of in vivo and in vitro experimental models of cardiac I/R injury (29–31). In addition, suppression of the cardiac electrogenic NBCe1 cotransporter reduces ischemic injury in the rat heart (32). Both transporters play a central role in the development of the reperfusion injury that

follows cardiac ischemia (32). The activities of both NHE1 and NBC are enhanced by various isozymes of carbonic anhydrase (CA), which bind to the transporters to form protein-protein complexes known as membrane transport metabolons (2, 35, 38, 42). CAs catalyze the reversible hydration of  $\text{CO}_2$  to provide the substrates for these transporters,  $\text{H}^+$  and  $\text{HCO}_3^-$ , respectively, and so maximize transmembrane ion transport activity. Furthermore, tissue CAs facilitate diffusion of  $\text{CO}_2$  from its site of production in the mitochondria to the bloodstream (18). In the heart, mitochondrial CAV, cytosolic CAII, and membrane-associated CAIV, CAIX, and CAXIV isozymes with their activity directed to the extracellular space have been detected (42, 51, 54–56). CA inhibitors have been previously used as diuretics targeting hypertension and heart failure (39). Furthermore, greater CA expression is a marker of the hypertrophic human heart, which can progress toward failure (3). We have identified CA inhibition as a means to intervene in the hypertrophic downward cascade of the failing heart by demonstrating that two potent CA inhibitors, benzolamide (BZ) and ethoxzolamide (ETZ), reduce cardiac dysfunction in rats subjected to permanent coronary artery ligation-induced myocardial infarction (56). In addition, it has been suggested that extracellular CA contributes more importantly than intracellular cytosolic CA isozymes to enhancing post-hypercarbic and global postischemic  $\text{pH}_i$  recovery of mammalian hearts (52). Thus, CA-catalyzed  $\text{CO}_2$  venting in the myocardium may be a contributor to cytosolic control of cardiac  $\text{pH}_i$  and useful to limit intracellular acidosis of poorly perfused microdomains (58).

Previous studies have shown that kinases such as p38 mitogen-activated protein kinase (MAPK), ERK1/2, and phosphatidylinositol 3-kinase (PI3K)/Akt, which are linked to ion transporters, are involved in cardioprotective pathways (21, 40). Furthermore, MAPK pathways of mammalian cells are stimulated by low environmental pH, oxidative, and other stresses (12). Phosphorylation of p38MAPK occurs in cardiomyocytes subjected to simulated ischemia (60). Moreover, inhibition of p38MAPK $\alpha$  isoform activation during ischemia (simulated ischemia with ischemia buffer) reduced injury and contributed to preconditioning-induced cardioprotection in a cultured rat cardiomyocyte model (49).

The first objective of the present study was to determine the effects of CA inhibition with the poorly membrane-diffusible CA inhibitor BZ on the outcomes from cardiac I/R, examining the participation of p38MAPK. Second, we compare the BZ-mediated actions with those obtained by the application of a brief acidic perfusion at the onset of reperfusion to mimic the transient acidosis status acquired by BZ.

## MATERIALS AND METHODS

Approval for the animal study was granted by the Animal Welfare Committee of the Faculty of Medicine, National University of La Plata [Comité Institucional para el Cuidado y Uso de los Animales de Laboratorio Facultad de Ciencias Médicas (CICUAL)]. All procedures in the present investigation conformed to the *Guide for the Care and Use of Laboratory Animals* published by the National Institutes of Health (NIH Pub. No. 85-23, updated 2011) and to the guidelines laid down by the CICUAL (Res. No. 209/13 Anexos I y II).

**Isolated heart preparation.** Wistar rats were anesthetized with ketamine (80 mg/kg) and diazepam (5 mg/kg) administered via intraperitoneal injections. Areflexia appearance with loss of corneal

reflex and the flexor reflex of escape in the lower limbs were verified before heart isolation and euthanasia. Hearts were quickly isolated and perfused with Tyrode solution containing (in mM) 118 NaCl, 5.9 KCl, 1.2  $\text{MgSO}_4$ , 1.35  $\text{CaCl}_2$ , 20  $\text{NaHCO}_3$ , and 11.0 glucose (gassed with 95%  $\text{O}_2$ -5%  $\text{CO}_2$ , pH 7.4, 37°C) with the Langendorff technique using a Masterflex Model 7016-21 perfusion pump (Cole-Parmer). The conductive tissue in the atrial septum was damaged with a fine needle to achieve atrioventricular block, and the right ventricle was paced at  $280 \pm 10$  beats/min. A latex balloon tied to the end of a polyethylene catheter was passed into the left ventricle (LV) through the mitral valve, and the opposite end was then connected to a Statham P23XL pressure transducer. The balloon was filled with water to provide a left ventricular end-diastolic pressure (LVEDP) of 8–12 mmHg, and this volume remained unchanged for the rest of the experiment. Coronary perfusion pressure was monitored at the point of cannulation of the aorta and was adjusted to ~60–70 mmHg. Coronary flow, which was controlled with a peristaltic pump, was  $11 \pm 2$  ml/min. Left ventricular developed pressure (LVDP) and its first derivative ( $\text{dP}/\text{dt}$ ) were recorded with a direct writing recorder.

**Experimental protocols.** After a 20-min stabilization period, the following experimental protocols were performed: 1) Nonischemic control (NIC) hearts ( $n = 8$ ) were perfused for 90 min without any treatment. 2) Ischemic control (IC) hearts ( $n = 6$ ) were subjected to 30 min of normothermic global ischemia followed by 60 min of reperfusion with a normal pH 7.4 buffer solution. Global ischemia was induced by stopping the perfusate inflow line, and the heart was placed in a saline bath held at 37°C. 3) BZ-treated hearts ( $n = 6$ ) were treated for 10 min at the beginning of reperfusion with 5  $\mu\text{M}$  BZ in the perfusion solution. The perfusion solution was maintained at pH 7.40. 4) Acidic reperfusion (AR) hearts ( $n = 6$ ) were perfused during the first 3 min of reperfusion with a buffer solution titrated to pH 6.4, followed by 57 min of reperfusion with a buffer solution of normal pH (7.4). The pH of the acidic solution was adjusted by lowering  $\text{HCO}_3^-$  concentration, maintaining the same gassing mixture (24).

All protocols were repeated in the presence of the p38MAPK inhibitor SB202190 (10  $\mu\text{M}$ ;  $n = 6$  for each one), a selective inhibitor of p38MAPK $\alpha$  and p38MAPK $\beta$  isoforms, administered during the initial 10 min of reperfusion.

**Infarct size determination.** We determined infarct size with the triphenyltetrazolium chloride (TTC) technique, as previously described (16). Briefly, at the end of reperfusion, atrial and right ventricular tissues were excised and LV was frozen. The frozen LV was cut into six transverse slices, which were incubated for 5 min at 37°C in a 1% solution of TTC. To measure myocardial infarction, the slices were weighed and scanned. Infarcted (pale) and viable ischemic-reperfused (red) areas were measured by computed planimetry (Scion Image 1.62; Scion, Frederick, MD). Infarct weights were calculated as previously described (15). Infarct size was expressed as a percentage of total area (area at risk) (14).

**Systolic and diastolic function.** Systolic function was assessed by LVDP, which is calculated by subtracting LVEDP from the left ventricular pressure (LVP) peak values, and the maximal velocity of rise of LVP ( $+\text{dP}/\text{dt}_{\text{max}}$ ). Diastolic function was evaluated as the maximal velocity of decrease of LVP ( $-\text{dP}/\text{dt}_{\text{max}}$ ) and LVEDP values.

**Immunoblotting.** The LV was homogenized, and its cytosolic fraction was isolated by differential centrifugation. Briefly, the LV was homogenized in ice-cold RIPA buffer (300 mM sucrose, 1 mM DTT, 4 mM EGTA, 20 mM Tris pH 7.4, 1% Triton X-100, 10% protease cocktail, 25  $\mu\text{M}$  FNa, 1  $\mu\text{M}$  orthovanadate) and centrifuged at 12,000g for 15 min at 4°C. The supernatant proteins (60  $\mu\text{g}$ ) were resolved on SDS-PAGE and transferred to a PVDF membrane (2 h). Equal loading of samples was confirmed by Ponceau S staining. Membranes were blocked with 5% nonfat milk in Tris-buffered saline (pH 7.5) containing 0.1% Tween (TBS-T) and probed overnight at 4°C with antibodies (rabbit) to phosphorylated (p-)p38MAPK (1:

1,000; Santa Cruz Biotechnology), p-Akt (1:1,000; Santa Cruz Biotechnology), p-PKC $\epsilon$  (1:1,000; Millipore), bax (1:1,000; Santa Cruz Biotechnology), or bcl2 (1:1,000, Santa Cruz Biotechnology). The membranes were washed four times for 10 min in TBS-T before the addition of HRP-conjugated anti-rabbit secondary antibody (1:5,000; Santa Cruz Biotechnology), and protein bands were analyzed by a chemiluminescent system (ECL Plus; Amersham Biosciences). Total protein signal was used as a loading control.

**Determination of  $pH_i$  in rat papillary muscles.** Rats were anesthetized with ketamine (100 mg/kg ip) and diazepam (10 mg/kg ip). Hearts were rapidly removed, and the papillary muscles from the LV were isolated, mounted in a perfusion chamber, and loaded with 2',7'-bis-(2-carboxyethyl)-5(6)-carboxyfluorescein (BCECF, AM form) for 30 min (final concentration 5  $\mu$ mol/l) at room temperature, as previously described (55). To measure fluorescence emission from BCECF, excitation light from a 75-W xenon lamp was band-pass filtered alternatively at 440 and 495 nm and then transmitted to the muscles by a dichroic mirror (reflecting wavelengths, <510 nm) located beneath the microscope. Fluorescence emission was collected by the microscope objective ( $\times 10$ ) and transmitted through a band-pass filter at  $535 \pm 5$  nm to a photomultiplier (model R2693; Hamamatsu). A manual shutter was used to select sampling intervals (2 s every  $\sim 10$  s) during the experimental protocol. At the end of each experiment, BCECF emitted fluorescence was calibrated in vivo by the high  $K^+$ -nigericin method.

**Measurement of  $pH_i$  after acid loading.** Papillary muscles were superfused with a  $HCO_3^-$ -buffered solution that contained (in mM) 128.3 NaCl, 4.5 KCl, 1.35  $CaCl_2$ , 20.23  $NaHCO_3$ , 1.05  $MgSO_4$ , and 11 glucose, equilibrated with a 5%  $CO_2$ -95%  $O_2$  gas mixture. Experiments were performed in the presence of the NHE inhibitor HOE642 (10  $\mu$ M). Acute acid loading with the ammonium chloride prepulse technique was achieved by the addition of 20 mM  $NH_4Cl$  (10 min) followed by washout of the  $NH_4Cl$ . The  $pH_i$  recovery after provoked acid loading was recorded by fluorescence emission of the muscles in the control untreated state, in the presence of 5  $\mu$ M BZ, in the presence of 10  $\mu$ M SB202190, and in the presence of both 5  $\mu$ M BZ and 10  $\mu$ M SB202190.

**Isolation of rat heart mitochondria.** At the end of reperfusion, mitochondria were obtained by differential centrifugation, as previously described (17). Briefly, the LV was homogenized in ice-cold isolation solution (IS) consisting of (in mM) 75 sucrose, 225 mannitol, and 0.01 EGTA neutralized with Trizma buffer at pH 7.4. Tissue pieces were settled, and the entire supernatant was discarded. After addition of fresh IS (5 ml) and proteinase (0.8 mg, bacterial, type XXIV; Sigma), the mixture was transferred to a hand homogenizer. After two-step homogenization (7 min each with 5-ml addition of fresh), the homogenate was transferred to a polycarbonate centrifuge tube. After 5 min of 750g centrifugation to discard unbroken tissue and debris, the supernatant was centrifuged at 8,000g for 10 min to sediment the mitochondria. The mitochondrial pellet obtained was washed twice with IS and once with suspension solution (IS without EGTA) at 8,000g for 5 min each. Residue was washed and resuspended in a cold solution containing mannitol and sucrose. Mitochondrial protein concentration was evaluated by the Bradford method with bovine serum albumin as standard. Purity was determined by immunodetection of the mitochondrial voltage-dependent anion channel and by the absence of cytosolic glyceraldehyde-3-phosphate dehydrogenase (GAPDH) (data not shown).

**Mitochondrial swelling determination.** Mitochondrial swelling was measured as a decrease in the 90° light-scattering signal (LSD) induced by the addition of  $CaCl_2$  to a final concentration of 200  $\mu$ M, which promotes influx of solutes through the opened MPTP and decreases light scattering. After 5 min of preincubation at 37°C in a medium containing (in mM) 120 KCl, 20 MOPS, 10 Tris-HCl, and 5  $KH_2PO_4$  pH 7.4, 200  $\mu$ M  $CaCl_2$  was added, as previously described (57). LSD was detected with a temperature-controlled Aminco Bow-

man Series 2 spectrofluorometer operating with continuous stirring at excitation and emission wavelengths of 520 nm and was calculated for each sample as the difference between the values before and after the addition of  $CaCl_2$ .

**Mitochondrial calcium retention capacity measurement.** Calcium retention capacity (CRC) was defined here as the amount of  $Ca^{2+}$  required to trigger a massive  $Ca^{2+}$  release by isolated cardiac mitochondria, as shown previously (17). CRC was expressed as nanomoles of  $CaCl_2$  per milligram of mitochondrial proteins. Extramitochondrial  $Ca^{2+}$  concentration was recorded with 0.5  $\mu$ M Calcium Green-5N (Invitrogen, Carlsbad, CA) with excitation and emission wavelengths set at 506 and 532 nm, respectively. Isolated mitochondria (0.5 mg/ml) were suspended in 2 ml of buffer (in mM: 150 sucrose, 50 KCl, 2  $KHPO_4$ , and 5 succinate in 20 Tris-HCl, pH 7.4). After preincubation (300 s), successive pulses of 10  $\mu$ M  $CaCl_2$  were applied. After mitochondria  $Ca^{2+}$  overload, MPTP irreversible opening and  $Ca^{2+}$  concentration increases in the incubation medium were detected by the spectrofluorometer system.

**Mitochondrial membrane potential.** Mitochondrial potential changes were evaluated by measuring rhodamine-123 (RH-123) fluorescence quenching under the buffer described above containing 0.1  $\mu$ M RH-123. The experiment was performed by exciting RH-123 at 503 nm and detecting the fluorescence emission at 527 nm, as previously described (17). During the measurements, the reaction medium containing mitochondria (0.1 mg/ml) was continuously stirred. Mitochondrial membrane potential ( $\Delta\Psi_m$ ) was calculated according to the instructions previously detailed with the Nernst-Guggenheim equation (50). RH-123 uptake is proportional to  $\Delta\Psi_m$ ; thus, the rate of fluorescence quenching and the steady-state level of fluorescence decrease are also a function of the  $\Delta\Psi_m$ .

**Statistical analysis.** Data are expressed as means  $\pm$  SE. Statistical analysis was performed by one-way analysis of variance (ANOVA) followed by the Newman-Keuls test used for multiple comparisons among groups. Values of  $P < 0.05$  were considered to indicate statistical significance.

## RESULTS

**Effects of carbonic anhydrase inhibition on myocardial damage and p38MAPK phosphorylation after acute global myocardial infarction.** In nonischemic control hearts, infarct size was on the order of 2% of area at risk, which most likely reflects a minor damage of tissues during the isolated heart Langendorff technique procedure, while it was  $\sim 30\%$  when hearts were subjected to I/R. BZ (5  $\mu$ M) reduced infarct size to  $\sim 8\%$  (Fig. 1), an extent of protection similar to that observed with a brief interval of AR (see Fig. 2C). The beneficial effects of BZ and AR were abolished when p38MAPK was inhibited with 10  $\mu$ M SB202190 with a degree of infarction not different from the ischemic control group.

During the stabilization period the values of LVDP, LVEDP,  $+dP/dt_{max}$  and  $-dP/dt_{max}$  were similar for all experimental groups (Fig. 3). In nonischemic control hearts, during 90 min of continuous perfusion the hearts exhibited a small decrease in contractility without change in diastolic stiffness as assessed by LVEDP. Thirty minutes of global ischemia followed by 60 min of reperfusion markedly reduced the postischemic recovery of myocardial function. At the end of reperfusion, LVDP decreased to values of  $18 \pm 3\%$  from baseline. LVEDP increased, reaching a value of  $54 \pm 3$  mmHg at the end of the reperfusion period. Addition of the CA inhibitor BZ (5  $\mu$ M) at the beginning of reperfusion attenuated the hypercontracture and promoted a remarkable restoration of contractile parameters (LVDP,  $+dP/dt_{max}$ , and  $-dP/dt_{max}$ ) reaching values com-

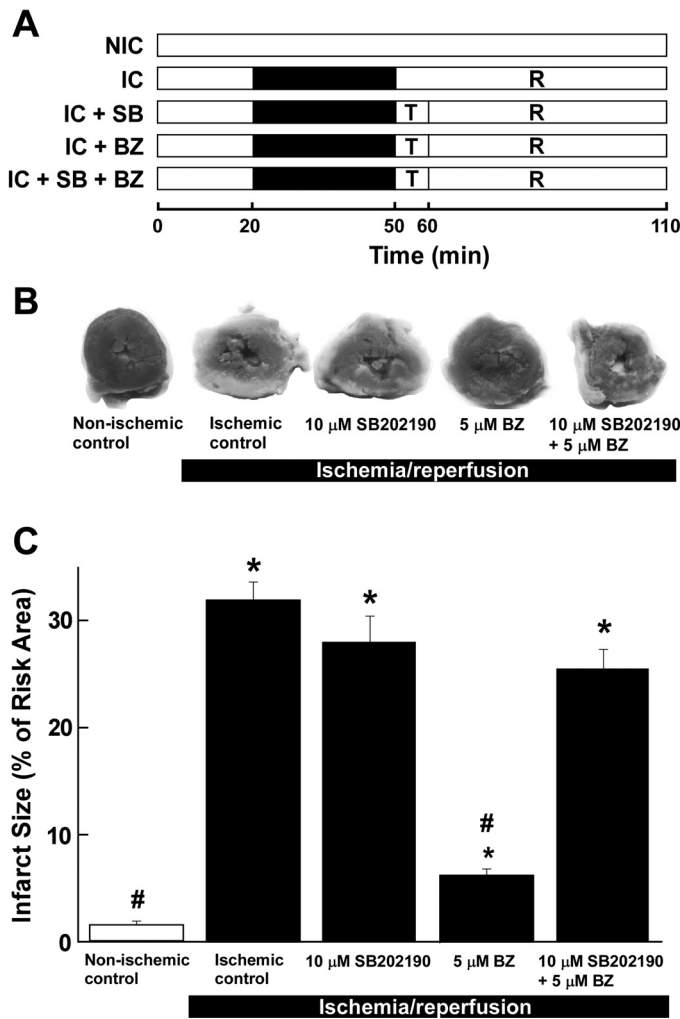


Fig. 1. Effect of CA and p38MAPK inhibition on myocardial injury after global ischemia. Isolated intact rat hearts were perfused for 90 min without any intervention or were subjected to 30 min of normothermic global ischemia followed by 60 min of reperfusion. *A*: schema of the different experimental groups. NIC, nonischemic control; IC, ischemic control; IC+SB, ischemic hearts perfused with p38MAPK inhibitor SB202190 (10 μM) during the first 10 min upon reperfusion; IC+BZ, ischemic hearts perfused with CA inhibitor BZ (5 μM) during the first 10 min upon reperfusion; IC+SB+BZ, ischemic hearts perfused with a combination of SB202190 (10 μM) and BZ (5 μM) during the first 10 min upon reperfusion; T, treatment; R, reperfusion. *B*: representative heart images of NIC, IC, IC+SB, IC+BZ, and IC+SB+BZ groups. Hearts were sectioned and stained with TTC to reveal infarcted tissue. Nonstained areas are indicative of infarct. *C*: infarct size was quantified from TTC-stained heart sections and expressed as % of risk area in NIC ( $n = 8$ ), IC ( $n = 6$ ), IC+SB ( $n = 6$ ), IC+BZ ( $n = 6$ ), and IC+SB+BZ ( $n = 5$ ). \* $P < 0.05$  vs. NIC; # $P < 0.05$  vs. IC.

parable to those acquired in nonischemic control hearts (Fig. 3). Hearts reperfused with buffer adjusted to pH 6.4 for the first 3 min also showed improved contractile force recovery (see Fig. 2*B*). Simultaneously, an attenuation of hypercontracture during reperfusion was obtained after the two interventions (BZ and AR) (Fig. 2*B* and Fig. 3). Our data also show that the blockade of p38MAPK prevented these beneficial actions elicited by CA inhibition (Fig. 3) and AR (Fig. 2*B*).

Mitogen-activated p38MAPK phosphorylation occurs in cardiomyocytes subjected to simulated ischemia (60). In our experimental conditions, at the end of the reperfusion period,

p-p38MAPK protein levels decreased by ~30% compared with nonischemic control hearts (Fig. 4, *A* and *B*). Conversely, the potent CA inhibitor BZ increased p-p38MAPK protein levels by 50%, and this increase was abrogated by SB202190 (Fig. 4, *A* and *B*). We also analyzed other upstream kinases implicated in phosphorylation cascades leading to activation of p38MAPK. Thus, in our experimental setting, p-Akt and

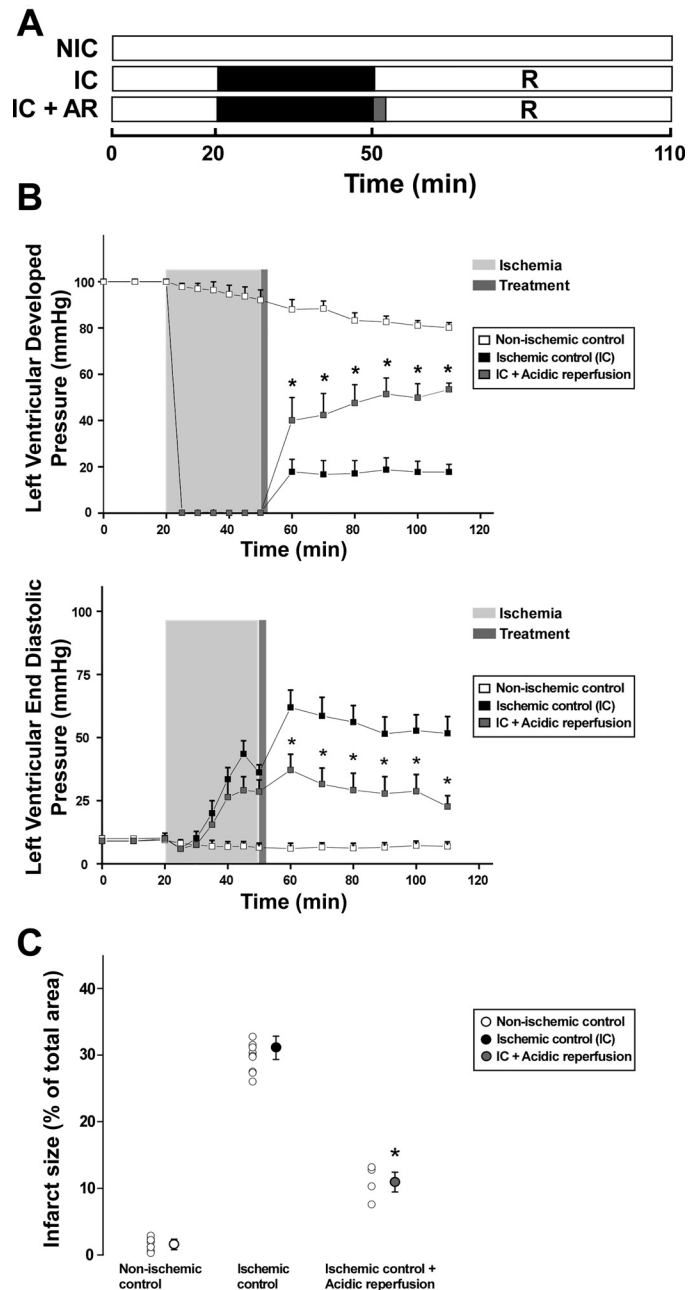
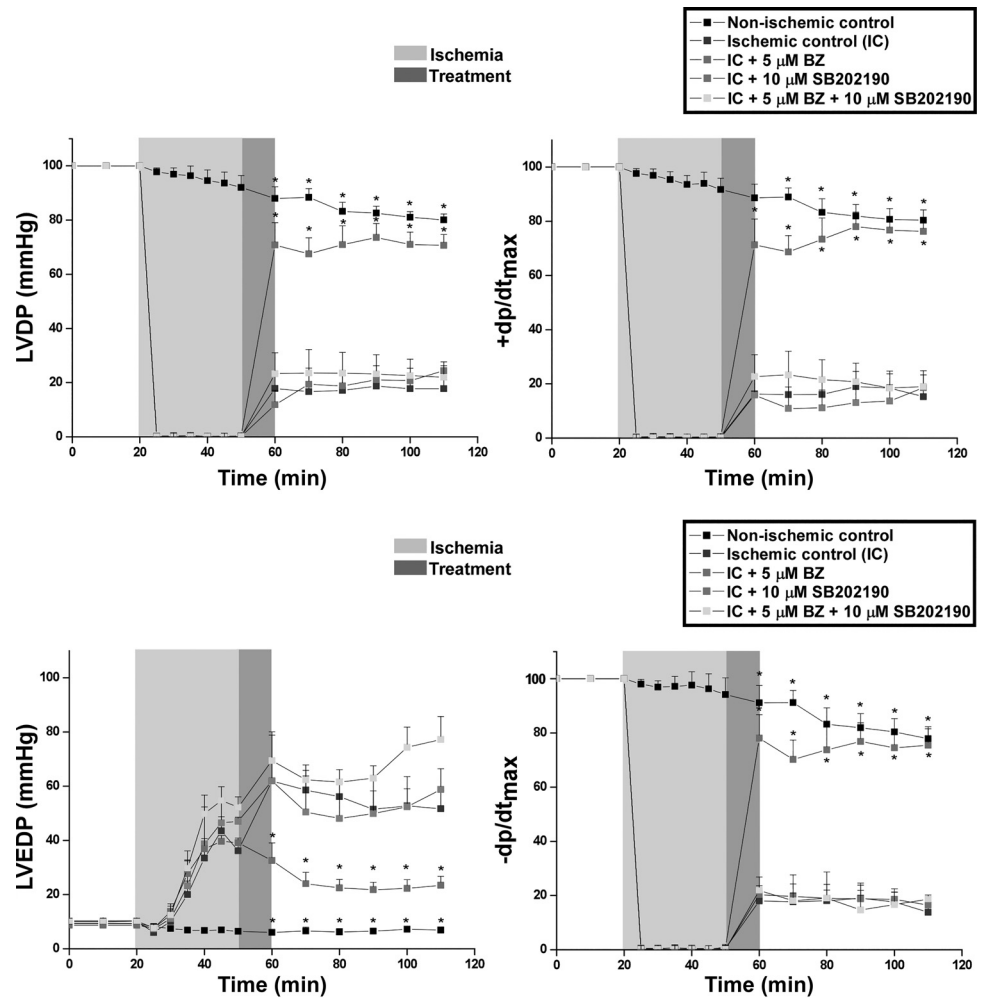


Fig. 2. Influence of perfusion with pH 6.4 buffer on myocardial injury. Isolated intact rat hearts were perfused for 90 min without any intervention or were subjected to 30 min of normothermic global ischemia followed by 60 min of reperfusion. *A*: schema of the different experimental groups. NIC, nonischemic control; IC, ischemic control; IC+AR, ischemic hearts perfused with pH 6.4 buffer for the first 3 min during reperfusion. *B*: time course of changes of left ventricular developed pressure (LVDP, top) and left ventricular end-diastolic pressure (LVEDP, bottom) in NIC ( $n = 8$ ), IC ( $n = 6$ ), and IC+AR ( $n = 6$ ). *C*: infarct size, expressed as % of risk area, in NIC ( $n = 6$ ), IC ( $n = 9$ ), and IC+AR ( $n = 4$ ). \* $P < 0.05$  vs. NIC.

Fig. 3. Influence of CA and p38MAPK inhibition on myocardial contractile performance after global ischemia. Isolated intact rat hearts were perfused for 90 min without any intervention or were subjected to 30 min of normothermic global ischemia followed by 60 min of reperfusion in the absence or presence of CA inhibitor BZ (5  $\mu$ M), the absence or presence of p38MAPK inhibitor SB202190 (10  $\mu$ M), or the combination of both BZ and SB20190. Time course of changes in left ventricular developed pressure (LVDP), maximal rise velocity of LVP ( $+dp/dt_{max}$ ), and maximal decrease velocity of LVP ( $-dp/dt_{max}$ ), expressed as % of preischemic values, and left ventricular end-diastolic pressure (LVEDP). \* $P < 0.05$  vs. IC.



p-PKC $\epsilon$  levels decreased in ischemic control hearts and increased in hearts treated with BZ (Fig. 4C). In a similar fashion, in ischemic hearts reperfused with acidic buffer we observed an increase in p-p38MAPK (Fig. 5A) and an increase in p-Akt and p-PKC $\epsilon$  (Fig. 5B), counteracting the decreased phosphorylation state of these kinases elicited by ischemia.

Taken together, the protection achieved by CA inhibition or short-term initial reperfusion of acidic buffer involves the activation of Akt-, PKC $\epsilon$ -, and p38MAPK-dependent pathways.

In parallel studies, the initial rate of  $pH_i$  recovery from an acute and transient acid loading was used to assess the activity of  $pH_i$  defense mechanisms involving  $HCO_3^-$  uptake by NBC cotransporters and acid extrusion by NHE-mediated  $Na^+/H^+$  exchange in isolated papillary muscles. Maximal induced acidification was of similar magnitude in all experimental groups (not shown). Under physiological conditions ( $HCO_3^-$  buffer),  $pH_i$  recovery was greater and faster, reaching steady-state conditions after 25 min (Fig. 6, A and B). The activity of NBC and NHE transporters is facilitated by CA, which rapidly provides  $H^+$  and  $HCO_3^-$  substrates to maximize transporter activity (2, 35, 36, 38, 42). The potent poorly membrane-permeant CA inhibitor BZ significantly inhibited  $pH_i$  recovery after transient acid loading:  $H^+$  efflux ( $J_{H^+}$ ) control values of

$0.43 \pm 0.08$  mM vs. BZ  $0.23 \pm 0.07$  mM measured at  $pH_i$  values of  $6.68 \pm 0.02$  and  $6.70 \pm 0.02$ , respectively (Fig. 6, A and B). Similarly, when experiments were performed in the presence of the NHE1 inhibitor HOE642 [cariporide, *N*-(aminomethyl)-4-(1-methylethyl)-3-(methylsulfonyl) benzamide], the recovery of  $pH_i$  after the acid loading was substantially reduced (Fig. 6, A and B). Thus, NHE1 activation accounts for  $\sim 75\%$  of the recovery after transient acid loading in papillary muscles superfused with  $HCO_3^-$  buffer. In addition, nearly 55% of the recovery after acidosis is dependent upon membrane-associated CA activity.

Sustained acidosis promotes MEK-ERK1/2-p90RS-mediated increases in NHE1 activity (13, 21). Here, we explored how transient acidosis and the CA inhibitor BZ affect p38MAPK-dependent recovery of  $pH_i$  after acid loading (Fig. 6, C and D). Experiments were performed in  $HCO_3^-$  buffer under blockade of NHE1 with HOE642. We found that BZ prolonged the acidic conditions with very slight  $pH_i$  recovery and reduction of  $J_{H^+}$  fluxes by 80% with BZ ( $0.02 \pm 0.02$  mM vs. control  $0.10 \pm 0.01$  mM; Fig. 6, C and D). The p38MAPK inhibitor SB202190 also significantly reduced the  $pH_i$  recovery after transient acidosis of HPMs. However, in the presence of BZ, inhibition of p38MAPK with SB202190 restored the ability of cardiac muscles to recover after transient acidosis, in

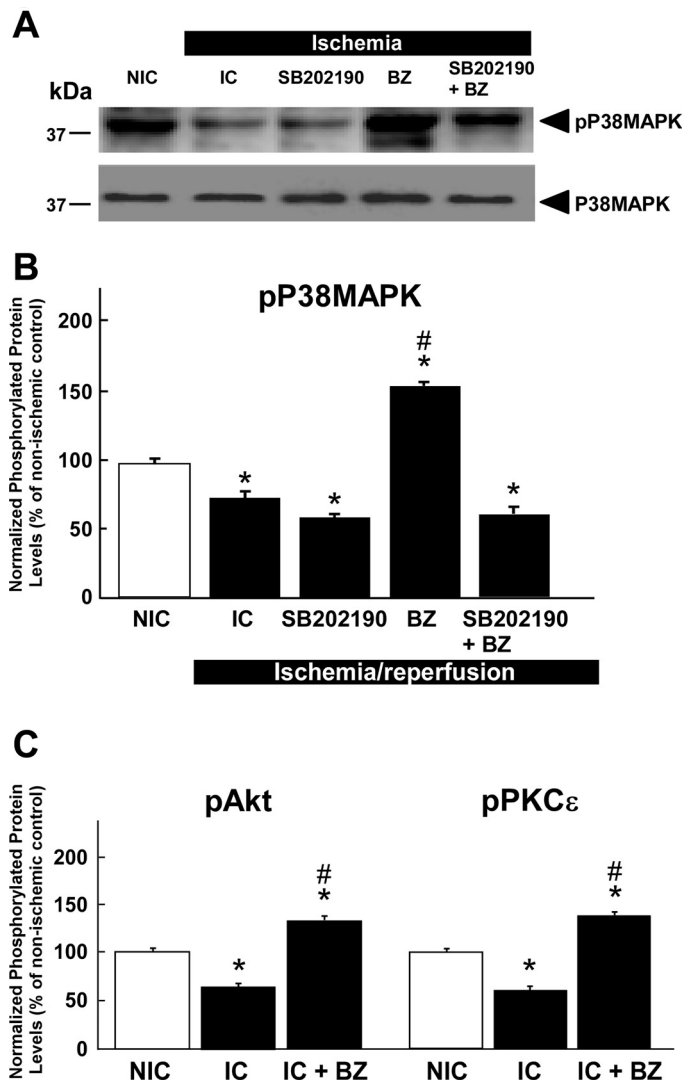


Fig. 4. Effect of CA inhibitor BZ on phosphorylated (p-)p38MAPK, p-Akt, and p-PKC $\epsilon$  protein levels. Left ventricle samples were collected at the end of the experimental protocols. Proteins (60  $\mu$ g) were resolved on SDS-PAGE, transferred to PVDF membrane, and probed with specific antibodies. *A*: representative immunoblots of p-p38MAPK (*top*), and p38MAPK (*bottom*), in NIC, IC, IC+SB, IC+BZ, and IC+SB+BZ groups. Arrowhead indicates position of proteins. *B*: densitometry analysis of p-p38MAPK, normalized to total p38MAPK protein levels and expressed as % of nonischemic control ( $n = 4$  for all groups). Experiments were performed in duplicate. \* $P < 0.05$  vs. NIC; # $P < 0.05$  vs. IC. *C*: expression of normalized p-Akt and p-PKC $\epsilon$ , expressed as % of nonischemic control. NIC, nonischemic control; IC, ischemic control; IC+BZ, ischemic control + BZ ( $n = 4$  for all groups). Experiments were performed in duplicate. \* $P < 0.05$  vs. NIC; # $P < 0.05$  vs. IC.

a similar manner to control (Fig. 6, *C* and *D*). Under these conditions, restoration of p38MAPK-mediated  $pH_i$  recovery could only be explained by other effects or targets of p38MAPK not explored in the present study, and this deserves further investigation.

We conclude that acidosis activates the p38MAPK pathway contributing to the  $HCO_3^-$ -dependent recovery of  $pH_i$ .

**Mitochondrial  $Ca^{2+}$  handling in infarcted hearts: effect of carbonic anhydrase inhibition.** Mitochondrial ultrastructural and functional injury occurs early in the course of ischemia and progresses during the ischemic period (34). Thus, mitochon-

drial perturbations contribute to cardiac dysfunction in I/R injury, and this mitochondrial failure comprises changes in the oxidative status of cardiac cells and abnormalities in mitochondrial  $Ca^{2+}$  handling, among others. To address potential mitochondrial protective effects of BZ-mediated acidification after reperfusion, we characterized the  $Ca^{2+}$  handling and changes of membrane potential ( $\Delta\Psi$ ) of mitochondria isolated from heart at the end of the I/R protocols as described in MATERIALS AND METHODS and presented in Fig. 1A and Fig. 2A.

Measurements of  $Ca^{2+}$ -induced mitochondrial swelling (MS) were evaluated in energized mitochondria isolated from LVs of hearts exposed to I/R. Heart mitochondrial suspensions were exposed to 200  $\mu$ M  $CaCl_2$  to induce MPTP opening with the consequent swelling. These changes were observed as LSD after addition of  $Ca^{2+}$  (not shown). LSD was significantly reduced in ischemic hearts compared with nonischemic controls, as previously shown (17) (Fig. 7A). Treatment with the p38MAPK inhibitor SB202190 did not further change the LSD in ischemic hearts. Notably, both short-term acidic perfusion (AR) and CA inhibition with BZ improved the response of mitochondria to  $Ca^{2+}$ , evidenced by greater LSD values than in ischemic control hearts. However, blockade of p38MAPK with SB202190 prevented the beneficial effects on MS produced by AR and BZ (Fig. 7A). Thus, MS and consequent MPTP opening in ischemic hearts are averted by preservation of acidic conditions achieved by AR or CA inhibition with BZ, in a mechanism that involves p38MAPK phosphorylation.

CRC, which is used as an indicator of the resistance of the MPTP to opening after mitochondrial matrix  $Ca^{2+}$  accumulation, was reduced in ischemic hearts compared with control, indicating significantly reduced  $Ca^{2+}$  tolerance in hearts exposed to ischemic stress (Fig. 7B). Conversely, CRC was preserved in ischemic hearts reperfused with AR or reperfused with BZ, and the effects of AR and BZ were abolished by inhibition of p38MAPK phosphorylation with SB202190.

Another signature of mitochondrial dysfunction is the preservation of  $\Delta\Psi_m$ , with a more depolarized state observed in stress-disturbed mitochondria. We measured rhodamine fluorescence changes in isolated mitochondria (not shown), following the ischemic protocols as above, and used observed changes for the membrane potential determination (Fig. 7C). The mean value of  $\Delta\Psi_m$  expressed in millivolts was significantly less negative in ischemic hearts compared with nonischemic controls, indicating that a more depolarized state predominates in organelles subjected to ischemic stress. After I/R  $\Psi_m$  also decreased in hearts treated with the p38MAPK inhibitor SB202190. AR or BZ attenuated the mitochondrial depolarization, with  $\Psi_m$  values not different from measurements obtained in nonischemic control hearts. However, SB202190 prevented restoration of  $\Psi_m$  attained by AR or BZ.

These data show that inhibition of CA with BZ improved the response to  $Ca^{2+}$  and the retention capacity of this ion simultaneously with  $\Delta\Psi_m$  normalization in hearts subjected to global ischemia and reperfusion. A similar result obtained with AR suggests that the cardiac postischemic mitochondrial dysfunction is prevented by early preservation of acidic conditions in a p-p38MAPK-dependent pathway.

Apoptosis contributes to myocardial infarct size and, depending on its relative contribution, acts to modulate postischemic functional recovery (5). Here, we determined by immunoblot analysis the contribution of apoptosis to myocardial

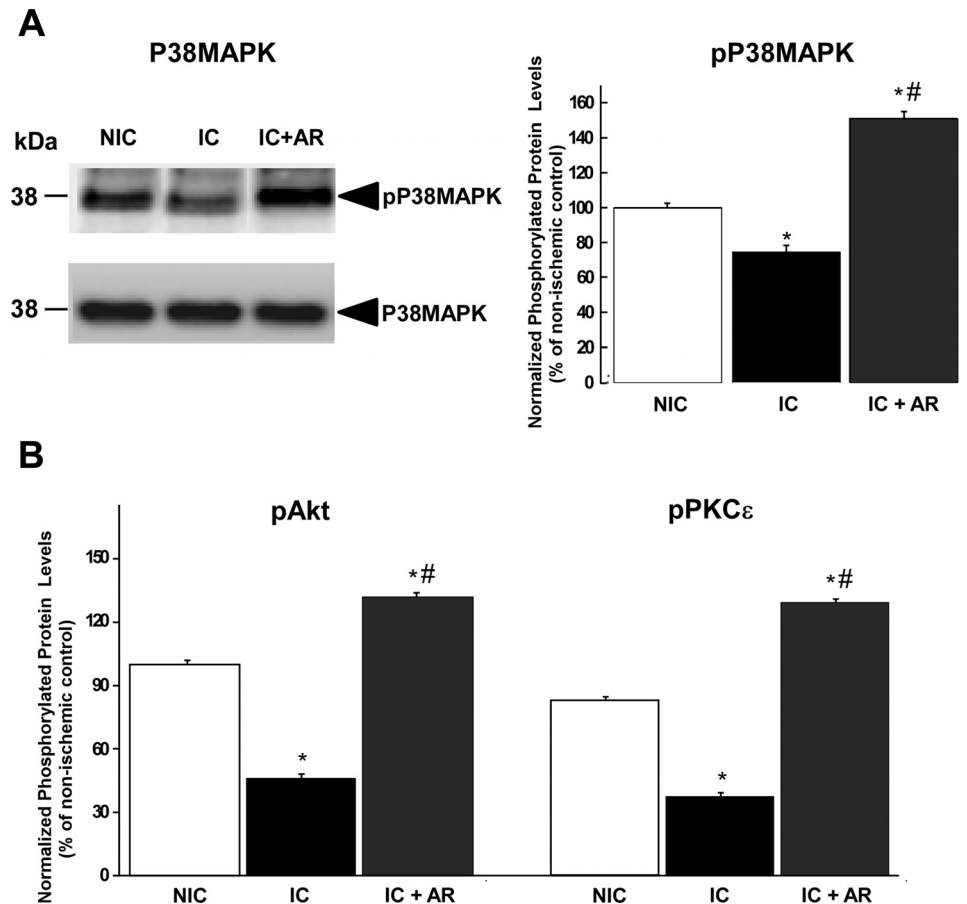


Fig. 5. Effect of acidic reperfusion on phosphorylated (p-)p38MAPK, p-Akt, and p-PKC $\epsilon$  protein levels. Left ventricle samples were collected at the end of the experimental protocols. Proteins (60  $\mu$ g) were resolved on SDS-PAGE, transferred to PVDF membrane, and probed with specific antibodies. **A**: p-p38MAPK normalized to total p38MAPK protein levels and expressed as % of nonischemic control. Arrowhead indicates position of proteins. **B**: normalized p-Akt and p-PKC $\epsilon$ , expressed as % of nonischemic control. NIC, nonischemic ( $n = 4$ ); IC, ischemic ( $n = 4$ ); IC+AR, ischemic + acidic reperfusion ( $n = 4$ ). Experiments were performed in duplicate. \* $P < 0.05$  vs. NIC; # $P < 0.05$  vs. IC.

injury and the effect of CA inhibition by BZ on the onset of this cell death event, using total heart homogenates. Antiapoptotic bcl2 protein decreased in ischemic hearts compared with control, in the presence or absence of the p38MAPK inhibitor SB202190 (Fig. 8, *A* and *B*). However, bcl2 expression in ischemic hearts treated with BZ was not different from nonischemic control, a condition reversed when BZ was applied in the presence of SB202190. The proapoptotic protein bax increased in ischemic hearts, or ischemic hearts receiving SB202190, but was slightly reduced when hearts were treated with BZ (Fig. 8, *A* and *B*); bax also increased in ischemic hearts reperfused with BZ in the presence of SB202190.

## DISCUSSION

The results of our study provide evidence that in the isolated rat heart subjected to global ischemia and reperfusion the protection afforded by the CA inhibitor BZ (given during the initial first 10 min of reperfusion) mimicked the beneficial effects observed when an acidic solution was applied initially during reperfusion. Furthermore, increased phosphorylation of p38MAPK occurs in ischemic control hearts reperfused in the presence of BZ or reperfused with acidic buffer. Our results also show that mitochondria from ischemic control hearts possess a reduced Ca<sup>2+</sup>-mediated response and CRC and a lower (more depolarized)  $\Delta\Psi_m$  than nonischemic control hearts. These mitochondrial changes were restored by treatment with BZ or AR but not when p38MAPK was inhibited. BZ also may reduce apoptosis in hearts subjected to ischemia,

as determined by the bax-to-bcl2 ratio. We suggest that prolongation of acidic conditions by membrane-bound CA inhibition protects the ischemic heart via a p38MAPK-dependent pathway leading to a preservation of mitochondrial function, a reduction of the infarct size, a reduction of cardiomyocyte apoptosis, and an improvement in contractile performance (Fig. 9).

Our data showing protection with both brief acidic reperfusion and BZ align with other studies using brief acidic reperfusion (47) and inhibition of H<sup>+</sup>-K<sup>+</sup>-ATPase by pantoprazole (7) and more deleterious effects when the perfusion fluid is equilibrated with 0% CO<sub>2</sub> (48).

Ischemic processes occurring in different tissues have been targeted pharmacologically with CA inhibitors. For instance, the CA inhibitor acetazolamide (ACTZ) reduced intracerebral hemorrhage-induced brain injury by reducing brain edema and neuronal death and improving functional outcome (19). ACTZ also reduced infarct volume and increased cerebral perfusion in a rat stroke model of transient middle cerebral artery occlusion (10). In addition, ACTZ exerted a protective role against I/R-induced acute kidney injury in an in vivo mouse model (4). More recently, treatment with ACTZ proved to be useful in protecting rat steatotic liver grafts against cold and normothermic I/R injuries (8, 9). In cardiac tissue, CA inhibitors prevent and reverse cardiomyocyte hypertrophic growth in cell culture models (1). More recently, in an in vivo rat model of prolonged myocardial infarction, CA inhibition with poorly membrane-diffusible BZ and membrane-permeant ETZ initiated after

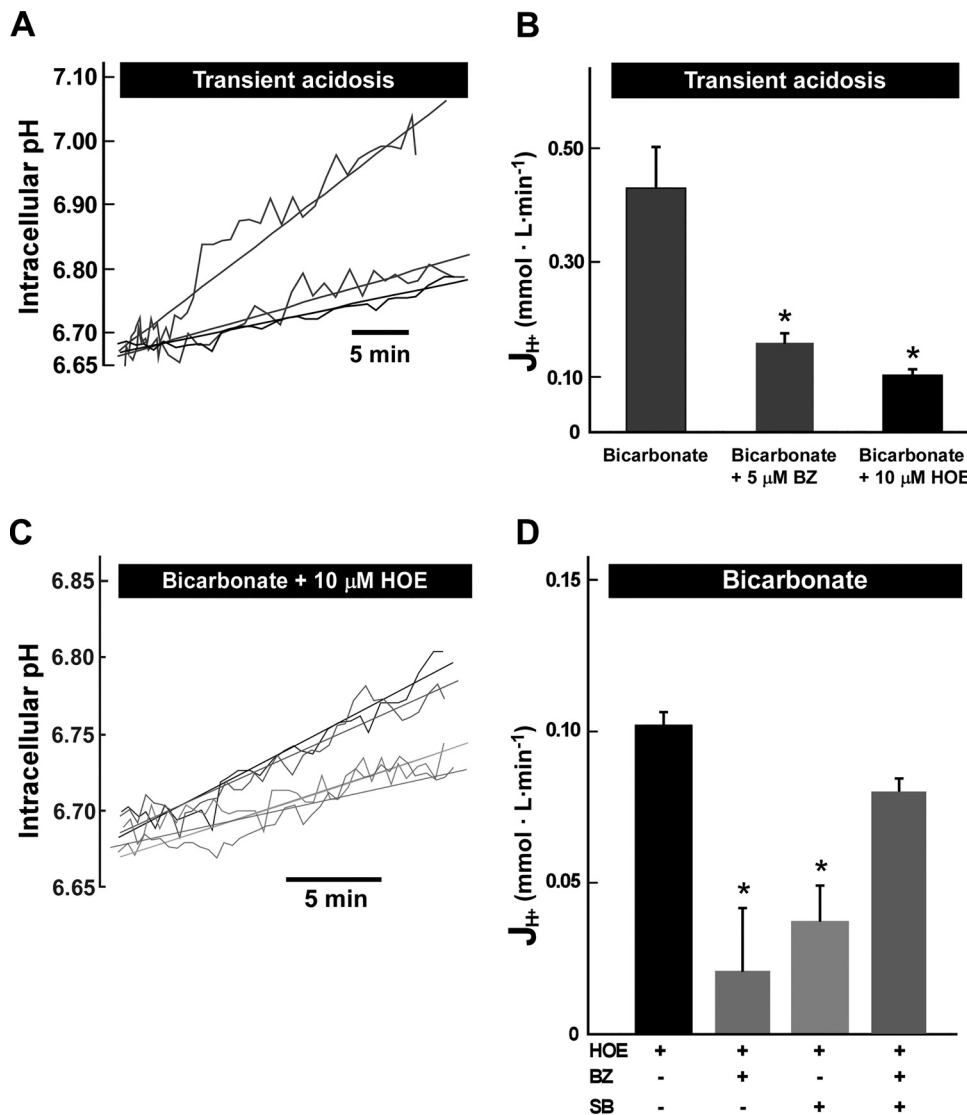


Fig. 6.  $pH_i$  recovery and effect of CA and p38MAPK inhibition on  $pH_i$  recovery after transient acidosis of isolated rat heart papillary muscles.  $pH_i$  was recorded after (non-sustained) transient acidosis induced by the ammonium prepulse technique in isolated papillary muscles. After imposed acid load, heart muscles were perfused with a bicarbonate buffer medium ( $CO_2/HCO_3^-$ ) and the average initial (maximal)  $H^+$  efflux ( $J_{H^+}$ ) was estimated after different treatments. **A**: representative  $pH_i$  recovery traces of papillary muscles perfused with bicarbonate (top trace), perfused with bicarbonate in the presence of BZ (5  $\mu M$ , middle trace), and perfused with bicarbonate in the presence of HOE642 (HOE) (10  $\mu M$ , bottom trace). **B**: summary of transport activity under all experimental conditions ( $n = 3$  for all groups). Average initial  $J_{H^+}$  was obtained after transient acidosis, compared at a similar maximal intracellular acidification among the groups.  $*P < 0.05$  vs. bicarbonate. **C**: bicarbonate-dependent  $pH_i$  recovery after ammonium prepulse-induced acid loading measured under blockade of the  $Na^+/H^+$  exchange activity with HOE (10  $\mu M$ ). Representative  $pH_i$  recovery traces after imposed transient acid loading of muscles perfused with bicarbonate (top trace), perfused with bicarbonate in the presence of BZ (5  $\mu M$ , bottom trace), perfused with bicarbonate in the presence of the p38MAPK inhibitor SB202190 (10  $\mu M$ , 3rd trace), or perfused with  $HCO_3^-$  in the presence of BZ and SB202190 (2nd trace). **D**: summary of transport activity under different experimental conditions ( $n = 3$  for all groups). Average initial  $J_{H^+}$  was obtained after transient acidosis, compared at a similar maximal intracellular acidification among the groups.  $*P < 0.05$  vs. bicarbonate+HOE.

establishment of heart failure improves cardiac function, limits interstitial fibrosis, and prevents LV remodeling (56). CAI, CAII, and CAIII expression has been detected in isolated bovine aortic smooth muscle, with particularly low expression levels and function accounted for these isozymes in mammalian vascular smooth muscle (VSM) (11). Thus, CA inhibition of the VSM present in coronary arteries, of the endothelium, and of the blood cells could all be other contributing factors for the observed beneficial effects of ETZ and BZ on ischemic heart processes.

Here, we demonstrated that inhibition of membrane-bound CA with BZ during I/R significantly reduces infarct size, prevents hypercontracture, and improves postischemic recovery of myocardial function. Similar results were observed in our studies when hearts were initially perfused with an acid solution, an intervention previously recognized as cardioprotective (24). In the present work, we also showed that BZ delays  $pH_i$  recovery of papillary muscles after transient acidosis, suggesting preservation of acidic conditions after CA inhibition. Based on this result, we can speculate that BZ perpetuates the acidosis generated during ischemia throughout

early reperfusion in the isolated rat heart. This speculation is supported by early observations showing that the CA inhibitors ETZ and BZ reduced the initial rates of  $pH_i$  after transient acidosis and caused a significant recovery of postischemic contractile function in Langendorff-perfused ferret hearts (52).

The question arising from our work is: What are the effects occurring when ischemic acidosis is prolonged in reperfusion? During the ischemic period, the more acidic  $pH_i$  generated by anaerobic metabolism activates two key intracellular alkalinizing mechanisms: NHE and NBC. Both NBC and NHE bind to the cytosolic enzyme CAII to form a transport metabolon. The catalytic activity of CAII ( $CO_2 + H_2O \leftrightarrow HCO_3^- + H^+$ ) produces  $HCO_3^-$  for influx and  $H^+$  for efflux by NBC and NHE, respectively. In addition, NBC binds to glycosylphosphatidylinositol-anchored CAIV (2) and transmembrane CAIX (42) in heart tissues. Our results in papillary muscles show that nearly 55% of  $pH_i$  recovery after transient acidosis depends upon membrane-associated CA activity, with NBC being the main (but perhaps not only) important mechanism, under these conditions of extracellular CA blockade. Therefore, the activity



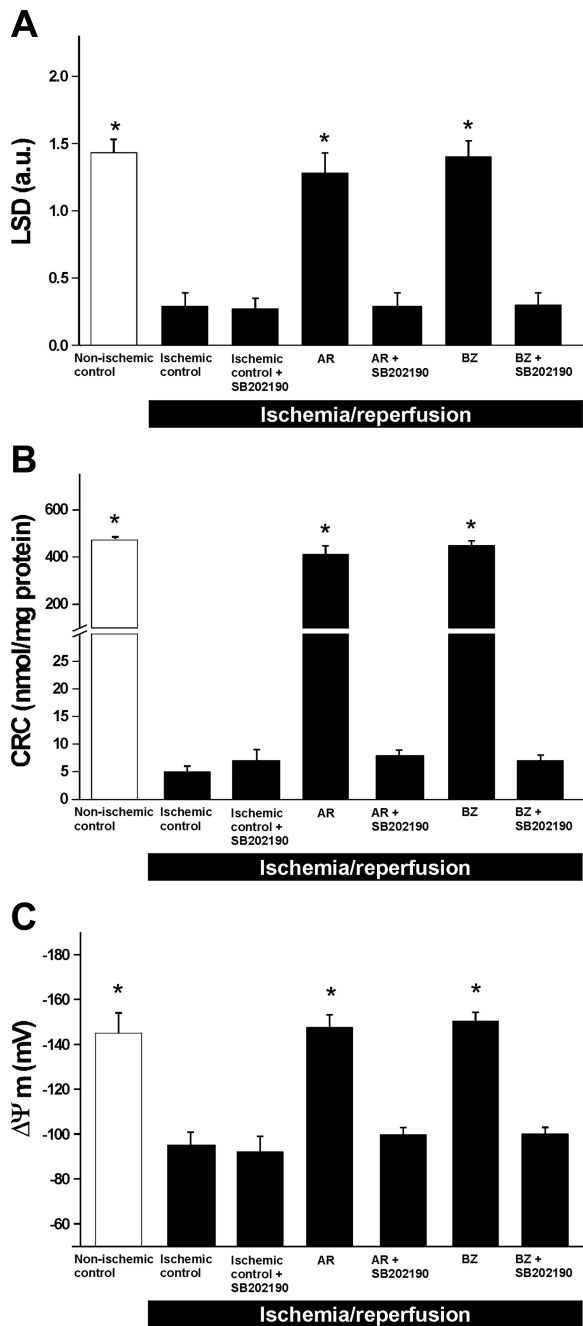


Fig. 7. Effect of acidic reperfusion and the CA inhibitor BZ on mitochondrial  $\text{Ca}^{2+}$  and mitochondrial membrane potential ( $\Delta\Psi_m$ ) after global ischemia. Mitochondria were isolated from rat hearts at the end of the ischemia-reperfusion according to the protocol described in MATERIALS AND METHODS and schemes displayed in Fig. 1A and Fig. 2A. A: mean values of light scattering decrease (LSD) in arbitrary units (a.u.) after the addition of 200  $\mu\text{M}$   $\text{Ca}^{2+}$  to samples of isolated mitochondria. B: mean values of  $\text{Ca}^{2+}$  retention capacity (CRC) in isolated mitochondria. C: mean values of  $\Delta\Psi_m$  measurement in isolated mitochondria: NIC ( $n = 4$ ), IC ( $n = 5$ ), IC+10  $\mu\text{M}$  SB202190 ( $n = 4$ ), IC+AR ( $n = 5$ ), IC+AR+10  $\mu\text{M}$  SB202190 ( $n = 4$ ), IC+5  $\mu\text{M}$  BZ ( $n = 4$ ), and IC+10  $\mu\text{M}$  SB202190+5  $\mu\text{M}$  BZ ( $n = 4$ );  $n =$  no. of hearts analyzed. Experiments on isolated mitochondria were run in duplicate. \* $P < 0.05$  vs. IC.

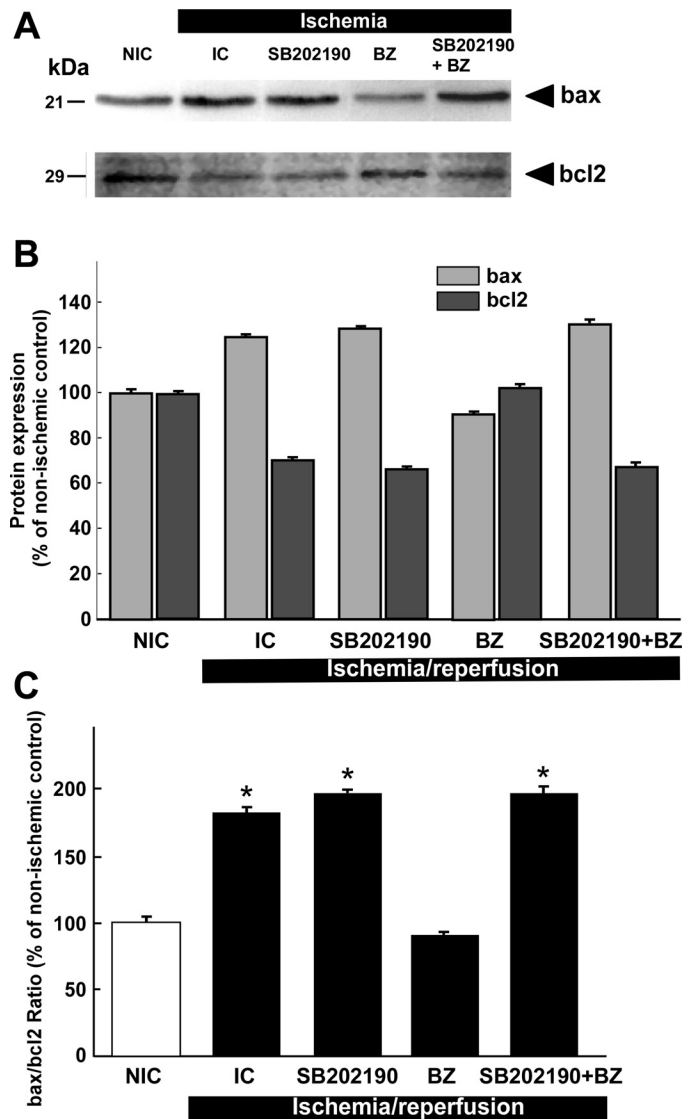


Fig. 8. Effect of CA inhibitor BZ on apoptotic protein levels. Left ventricle samples were collected at the end of the experimental protocols. Proteins (60  $\mu\text{g}$ ) were resolved on SDS-PAGE, transferred to PVDF membrane, and probed with specific antibodies. A: representative immunoblots of bax (top) and bcl2 (bottom) in NIC, IC, IC+SB, IC+BZ, and IC+SB+BZ groups. Arrowhead indicates position of proteins. B: densitometry analysis of bax and bcl2 (arbitrary units) expressed as % of nonischemic control. C: densitometry analysis of bax-to-bcl2 ratio (arbitrary units) expressed as % of nonischemic control. NIC, nonischemic control; IC, ischemic control; IC+SB, ischemic control + 10  $\mu\text{M}$  SB202190; IC+BZ, ischemic control + 5  $\mu\text{M}$  BZ; IC+SB+BZ, ischemic control + 10  $\mu\text{M}$  SB202190 + 5  $\mu\text{M}$  BZ ( $n = 2$  for all groups). Experiments were performed in duplicate. \* $P < 0.05$  vs. NIC.

of both transporters (NHE and NBC) is attenuated by BZ and so contributes to generation of a more acidic environment. Additionally, increased activity of NHE and NBC and the energetic failure of  $\text{Na}^+$ -ATPase lead to intracellular  $\text{Na}^+$  accumulation and secondarily to greater  $\text{Na}^+/\text{Ca}^{2+}$  exchange-mediated elevation in intracellular  $\text{Ca}^{2+}$ . During reperfusion, NHE and NBC contribute to  $\text{Na}^+$  and  $\text{Ca}^{2+}$  overloading (53). Thus, delaying  $\text{pH}_i$  normalization or maintaining a low  $\text{pH}$  protects the heart (25, 26, 46) and favorably maintains cation homeostasis as demonstrated by reduction of intracellular  $\text{Na}^+$  and  $\text{Ca}^{2+}$  overload (43). However, this window of protection is

lost when NHE and NBC transport activities quickly return to their maximal capacity upon reperfusion and washout of  $\text{CO}_2$  and acidic metabolites, as suggested previously (24).

Preservation of mitochondrial function after I/R is critical to survival of the myocardium (22).  $\text{Ca}^{2+}$  overload and reactive oxygen species generation participate in the formation and opening of the MPTP, which plays an important role in cardiac cell death (23). When there is irreversible MPTP opening, a collapse of the membrane potential occurs, accompanied by uncoupling of the respiratory electron transport chain, swelling

of the organelle, and concomitant release of cytochrome *c* and other proapoptotic factors. All of these result in apoptotic or necrotic cell death (23). Contractile dysfunction of the ischemic heart correlates with the extent of MPTP opening. Inhibition of MPTP provides protection by reducing  $\text{Ca}^{2+}$  overload or reactive oxygen species generation or by lowering the  $\text{pH}_i$  (20, 25). Moreover, inhibition of mitochondrial NHE1 reduced MPTP opening and mitochondrial swelling of isolated heart mitochondria (59) and changed mitochondrial fission-fusion protein dynamics affected by postinfarction remodeling (27). Recently, it was demonstrated that  $\text{Ca}^{2+}$ -induced MPTP opening and consequent mitochondrial swelling was attenuated by the NHE1 inhibitor cariporide in isolated rat heart mitochondria (57), as previously shown (59). Furthermore, the same study proved that acidic buffer conditions protected heart mitochondria, as indicated by a decreased susceptibility to opening of the MPTP provoked by high  $\text{Ca}^{2+}$  concentration. Interestingly, the NBCn1  $\text{Na}^+$ - $\text{HCO}_3^-$  cotransporter, which is expressed in heart mitochondria, plays a functional role to prevent MPTP opening and subsequent volume increase when mitochondria are exposed to high  $\text{Ca}^{2+}$  (57).

Additionally, cardioprotective signaling relies on increased phosphorylation of certain proteins which regulates the onset of myocardial cell injury. Major protein kinase pathways activated by myocardial I/R include PKC isoforms, MAP kinases, ERK1/2, JNK1/2, p38MAPK, cell survival PI3K/Akt, p90RSK, and tyrosine kinases (6). In the present study, we found reduced phosphorylation of p38MAPK, PKC $\epsilon$ , and Akt after 30 min of global ischemia and 60 min of reperfusion in isolated intact rat hearts. However, when hearts were perfused initially with BZ or acidic buffer for short periods, increased phosphorylation of p38MAPK, Akt, and PKC $\epsilon$  occurred. Previously, it was demonstrated that intracellular acidification activates p38MAPK independently from changes in extracellular pH (61). Therefore, in our experimental conditions the perpetuation of ischemic acidosis during the first minutes of reperfusion could be one possible mechanism to explain the increase in p38MAPK phosphorylation detected in BZ and AR groups. Our results in papillary muscle provide evidence that BZ maintains a more acidic pH. If this event takes place at the beginning of reperfusion in isolated heart, activation of alkalinizing mechanisms would be slowed, leading to a diminution of  $\text{Ca}^{2+}$  concentration and attenuation of  $\text{Ca}^{2+}$ -dependent signaling pathways. Calcineurin is a serine/threonine phospho-

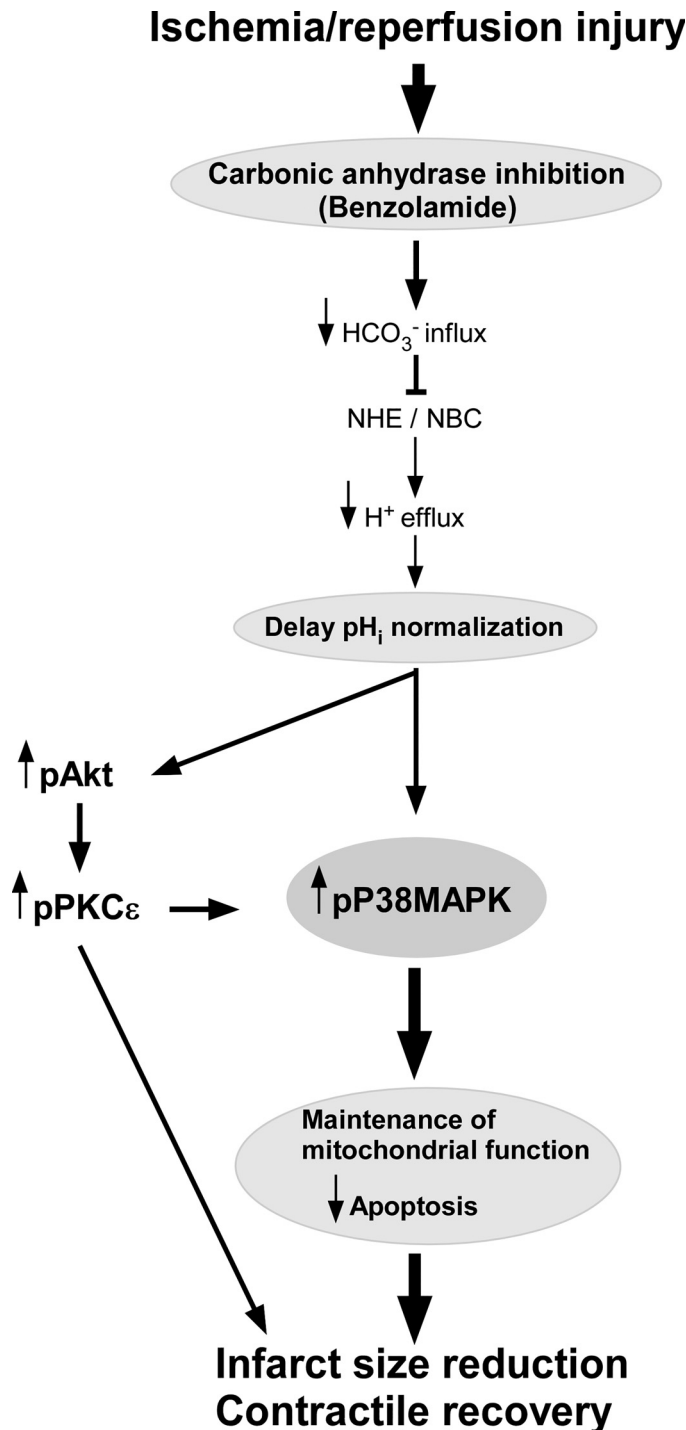


Fig. 9. Scheme showing the proposed mechanisms of cardioprotection elicited by carbonic anhydrase (CA) inhibitor BZ after global acute myocardial infarction injury. In isolated rat heart subjected to global ischemia (which causes myocardial injury), the protection achieved by CA inhibitor BZ involves a delay of  $\text{pH}_i$  normalization or maintenance of low  $\text{pH}$  by reduced  $\text{Na}^+$ / $\text{H}^+$  exchanger (NHE) and  $\text{Na}^+$ - $\text{HCO}_3^-$  cotransporter (NBC) activities. BZ would decrease  $\text{HCO}_3^-$  at the extracellular cardiomyocyte domain and thus its influx, with resultant reduced  $\text{H}^+$  efflux from the cell via NHE1 and NBC. BZ would then maintain  $\text{pH}_i$  in transient acidotic state (for a brief period). Increased phosphorylation of the p38MAPK pathway occurs in ischemic hearts reperfused in the presence of BZ, preventing mitochondrial dysfunction and reduction of apoptosis. Prolongation of acidic conditions by membrane-bound CA inhibition (with BZ) protects the ischemic heart via a p38MAPK-dependent pathway leading to a reduction of the infarct size and increased contractility of the injured heart. Delay of  $\text{pH}_i$  normalization upon BZ-mediated CA inhibition also increases Akt and PKC $\epsilon$  phosphorylation, projecting beneficial effects on hearts exposed to myocardial infarction.

tase activated by  $\text{Ca}^{2+}$  that participates in p38MAPK inactivation (37). Therefore, we could speculate that BZ- and AR-induced increase of p38MAPK phosphorylation could result from the inactivation of calcineurin in response to decreased intracellular  $\text{Ca}^{2+}$  levels. However, we cannot rule out that CA inhibition may affect other pathways involving different kinases, such as the PI3K-Akt-eNOS signaling pathway (47).

Apoptosis is a distinct pathway contributing to myocardial damage following ischemia and reperfusion (5). We have shown that BZ favorably alters the bax-to-bcl-2 ratio, which can act as a rheostat and determine cellular susceptibility to apoptosis. Lower levels of this ratio may lead to resistance of cardiomyocytes to apoptosis, when hearts are subjected to an ischemic insult. We observed an increase in bax/bcl2 in ischemic hearts that was prevented by the CA inhibitor BZ, inferring heart protection, and this protection was lost in the presence of the p38MAPK inhibitor SB202190 as demonstrated by increased bax/bcl2 (Fig. 8C). We suggest that BZ attenuates cardiomyocyte apoptosis following myocardial infarction and that this beneficial effect of CA inhibition is mediated through a p38MAPK-dependent pathway. The induction and final commitment of the apoptosis pathways to irreversible myocardial injury can be modulated with the use of different inhibitors, as shown in I/R rat hearts (41). Our results indicate that the ischemia-induced apoptosis of isolated perfused rat hearts can be significantly decreased by the CA inhibitor BZ during early reperfusion, but this protection is only achieved when p38MAPK is activated, presumably via a BZ-promoted transient acidotic preservation in myocardial tissue.

We conclude that CA inhibitors in general and membrane-impermeant BZ in particular exert beneficial effects on myocardium subjected to I/R. BZ decreased apoptosis, decreased infarct size and postischemic myocardial dysfunction, and ameliorated mitochondrial alterations. These actions appear to be mediated by a reduction of  $\text{Ca}^{2+}$  overload through low  $\text{pH}_i$ -mediated p38MAPK activation and pathways that involve the participation of Akt and PKC $\epsilon$ . Our data strongly support the possibility that CA blockade by BZ or other CA inhibitors might be a practical and effective therapeutic option in the treatment of acute cardiac I/R injury.

#### ACKNOWLEDGMENTS

R. G. Díaz, L. F. González Arbeláez, N. G. Pérez, S. M. Mosca, and B. V. Alvarez are Established Investigators of the Consejo Nacional de Investigaciones Científicas y Tecnológicas (CONICET, Argentina). A. Ciocci Pardo was supported by a Fellowship from CONICET.

#### GRANTS

This work was supported by PICT 2013 No. 01976 (FONCyT, Argentina) Grant to B. V. Alvarez.

#### DISCLOSURES

No conflicts of interest, financial or otherwise, are declared by the authors.

#### AUTHOR CONTRIBUTIONS

A.C.P., R.G.D., and L.F.G.A. performed experiments; A.C.P., R.G.D., L.F.G.A., S.M.M., and B.V.A. analyzed data; A.C.P., R.G.D., L.F.G.A., S.M.M., and B.V.A. interpreted results of experiments; A.C.P., R.G.D., and L.F.G.A. prepared figures; N.G.P., S.M.M., and B.V.A. conceived and designed research; N.G.P., E.R.S., S.M.M., and B.V.A. edited and revised manuscript; B.V.A. drafted manuscript; B.V.A. approved final version of manuscript.

#### REFERENCES

- Alvarez BV, Johnson DE, Sowah D, Soliman D, Light PE, Xia Y, Karmazyn M, Casey JR. Carbonic anhydrase inhibition prevents and reverses cardiomyocyte hypertrophy. *J Physiol* 579: 127–145, 2007. doi:10.1113/jphysiol.2006.123638.
- Alvarez BV, Loisele FB, Supuran CT, Schwartz GJ, Casey JR. Direct extracellular interaction between carbonic anhydrase IV and the human NBC1 sodium/bicarbonate co-transporter. *Biochemistry* 42: 12321–12329, 2003. doi:10.1021/bi0353124.
- Alvarez BV, Quon AL, Mullen J, Casey JR. Quantification of carbonic anhydrase gene expression in ventricle of hypertrophic and failing human heart. *BMC Cardiovasc Disord* 13: 2, 2013. doi:10.1186/1471-2261-13-2.
- An Y, Zhang JZ, Han J, Yang HP, Tie L, Yang XY, Xiaokaiti Y, Pan Y, Li XJ. Hypoxia-inducible factor-1 $\alpha$  dependent pathways mediate the renoprotective role of acetazolamide against renal ischemia-reperfusion injury. *Cell Physiol Biochem* 32: 1151–1166, 2013. doi:10.1159/000354515.
- Anversa P, Cheng W, Liu Y, Leri A, Redaelli G, Kajstura J. Apoptosis and myocardial infarction. *Basic Res Cardiol* 93, Suppl 3: 8–12, 1998. doi:10.1007/s003950050195.
- Armstrong SC. Protein kinase activation and myocardial ischemia/reperfusion injury. *Cardiovasc Res* 61: 427–436, 2004. doi:10.1016/j.cardiores.2003.09.031.
- Bacaksiz A, Teker ME, Buyukpinarbasili N, Inan O, Tasal A, Sonmez O, Erdogan E, Turfan M, Akdemir OC, Ertas G. Does pantoprazole protect against reperfusion injury following myocardial ischemia in rats? *Eur Rev Med Pharmacol Sci* 17: 269–275, 2013.
- Bejaoui M, Pantazi E, De Luca V, Panisello A, Folch-Puy E, Hotter G, Capasso C, Supuran CT, Roselló-Catafau J. Correction: Carbonic anhydrase protects fatty liver grafts against ischemic reperfusion damage. *PLoS One* 10: e0139411, 2015. doi:10.1371/journal.pone.0139411.
- Bejaoui M, Pantazi E, De Luca V, Panisello A, Folch-Puy E, Serafin A, Capasso C, Supuran CT, Roselló-Catafau J. Acetazolamide protects steatotic liver grafts against cold ischemia reperfusion injury. *J Pharmacol Exp Ther* 355: 191–198, 2015. doi:10.1124/jpet.115.225177.
- Beretta S, Versace A, Carone D, Riva M, Dell’Era V, Cuccione E, Cai R, Monza L, Pirovano S, Padovano G, Stirop F, Presotto L, Paterno G, Rossi E, Giussani C, Sganzerla EP, Ferrarese C. Cerebral collateral therapeutics in acute ischemic stroke: a randomized preclinical trial of four modulation strategies. *J Cereb Blood Flow Metab* 37: 3344–3354, 2017. doi:10.1177/0271678X16688705.
- Berg JT, Ramanathan S, Gabrielli MG, Swenson ER. Carbonic anhydrase in mammalian vascular smooth muscle. *J Histochem Cytochem* 52: 1101–1106, 2004. doi:10.1369/jhc.4A6266.2004.
- Clerk A, Michael A, Sugden PH. Stimulation of multiple mitogen-activated protein kinase sub-families by oxidative stress and phosphorylation of the small heat shock protein, HSP25/27, in neonatal ventricular myocytes. *Biochem J* 333: 581–589, 1998. doi:10.1042/bj3330581.
- Díaz RG, Nolly MB, Massarutti C, Casarini MJ, Garcarena CD, Ennis IL, Cingolani HE, Pérez NG. Phosphodiesterase 5A inhibition decreases NHE-1 activity without altering steady state  $\text{pH}_i$ : role of phosphatases. *Cell Physiol Biochem* 26: 531–540, 2010. doi:10.1159/000322321.
- Fantinelli JC, González Arbeláez LF, Pérez Núñez IA, Mosca SM. Protective effects of *N*-(2-mercaptopropionyl)-glycine against ischemia-reperfusion injury in hypertrophied hearts. *Exp Mol Pathol* 94: 277–284, 2013. doi:10.1016/j.yexmp.2012.07.004.
- Fantinelli JC, Orłowski A, Aiello EA, Mosca SM. The electrogenic cardiac sodium bicarbonate co-transporter (NBCe1) contributes to the reperfusion injury. *Cardiovasc Pathol* 23: 224–230, 2014. doi:10.1016/j.carpath.2014.03.003.
- Ferrera R, Benhabbouche S, Bopassa JC, Li B, Ovize M. One hour reperfusion is enough to assess function and infarct size with TTC staining in Langendorff rat model. *Cardiovasc Drugs Ther* 23: 327–331, 2009. doi:10.1007/s10557-009-6176-5.
- González Arbeláez LF, Ciocci Pardo A, Fantinelli JC, Caldiz C, Ríos JL, Schinella GR, Mosca SM. Ex vivo treatment with a polyphenol-enriched cocoa extract ameliorates myocardial infarct and postischemic mitochondrial injury in normotensive and hypertensive rats. *J Agric Food Chem* 64: 5180–5187, 2016. doi:10.1021/acs.jafc.6b01669.
- Gros G, Moll W, Hoppe H, Gros H. Proton transport by phosphate diffusion—a mechanism of facilitated  $\text{CO}_2$  transfer. *J Gen Physiol* 67: 773–790, 1976. doi:10.1085/jgp.67.6.773.

19. Guo F, Hua Y, Wang J, Keep RF, Xi G. Inhibition of carbonic anhydrase reduces brain injury after intracerebral hemorrhage. *Transl Stroke Res* 3: 130–137, 2012. doi:10.1007/s12975-011-0106-0.
20. Halestrap AP, Clarke SJ, Javadov SA. Mitochondrial permeability transition pore opening during myocardial reperfusion—a target for cardioprotection. *Cardiovasc Res* 61: 372–385, 2004. doi:10.1016/S0008-6363(03)00533-9.
21. Haworth RS, McCann C, Snabaitis AK, Roberts NA, Avkiran M. Stimulation of the plasma membrane Na<sup>+</sup>/H<sup>+</sup> exchanger NHE1 by sustained intracellular acidosis. Evidence for a novel mechanism mediated by the ERK pathway. *J Biol Chem* 278: 31676–31684, 2003. doi:10.1074/jbc.M304400200.
22. Heusch G, Boengler K, Schulz R. Cardioprotection: nitric oxide, protein kinases, and mitochondria. *Circulation* 118: 1915–1919, 2008. doi:10.1161/CIRCULATIONAHA.108.805242.
23. Heusch G, Boengler K, Schulz R. Inhibition of mitochondrial permeability transition pore opening: the Holy Grail of cardioprotection. *Basic Res Cardiol* 105: 151–154, 2010. doi:10.1007/s00395-009-0080-9.
24. Inserte J, Barba I, Hernando V, Abellán A, Ruiz-Meana M, Rodríguez-Sinovas A, García-Dorado D. Effect of acidic reperfusion on prolongation of intracellular acidosis and myocardial salvage. *Cardiovasc Res* 77: 782–790, 2008. doi:10.1093/cvr/cvm082.
25. Inserte J, Barba I, Poncelas-Nozal M, Hernando V, Agulló L, Ruiz-Meana M, García-Dorado D. cGMP/PKG pathway mediates myocardial postconditioning protection in rat hearts by delaying normalization of intracellular acidosis during reperfusion. *J Mol Cell Cardiol* 50: 903–909, 2011. doi:10.1016/j.yjmcc.2011.02.013.
26. Inserte J, Ruiz-Meana M, Rodríguez-Sinovas A, Barba I, García-Dorado D. Contribution of delayed intracellular pH recovery to ischemic postconditioning protection. *Antioxid Redox Signal* 14: 923–939, 2011. doi:10.1089/ars.2010.3312.
27. Javadov S, Huang C, Kirshenbaum L, Karmazyn M. NHE-1 inhibition improves impaired mitochondrial permeability transition and respiratory function during postinfarction remodeling in the rat. *J Mol Cell Cardiol* 38: 135–143, 2005. doi:10.1016/j.yjmcc.2004.10.007.
28. Kaplan SH, Yang H, Gilliam DE, Shen J, Lemasters JJ, Cascio WE. Hypercapnic acidosis and dimethyl amiloride reduce reperfusion induced cell death in ischaemic ventricular myocardium. *Cardiovasc Res* 29: 231–238, 1995. doi:10.1016/S0008-6363(96)88575-0.
29. Karmazyn M. Mechanisms of protection of the ischemic and reperfused myocardium by sodium-hydrogen exchange inhibition. *J Thromb Thrombolysis* 8: 33–38, 1999. doi:10.1023/A:1008990530176.
30. Karmazyn M. Pharmacology and clinical assessment of cariporide for the treatment coronary artery diseases. *Expert Opin Investig Drugs* 9: 1099–1108, 2000. doi:10.1517/13543784.9.5.1099.
31. Karmazyn M, Sostaric JV, Gan XT. The myocardial Na<sup>+</sup>/H<sup>+</sup> exchanger: a potential therapeutic target for the prevention of myocardial ischaemic and reperfusion injury and attenuation of postinfarction heart failure. *Drugs* 61: 375–389, 2001. doi:10.2165/00003495-200161030-00006.
32. Khandoudi N, Albadine J, Robert P, Krief S, Berrebi-Bertrand I, Martin X, Bevensee MO, Boron WF, Bril A. Inhibition of the cardiac electrogenic sodium bicarbonate cotransporter reduces ischemic injury. *Cardiovasc Res* 52: 387–396, 2001. doi:10.1016/S0008-6363(01)00430-8.
33. Lemasters JJ, Bond JM, Chacon E, Harper IS, Kaplan SH, Ohata H, Trollinger DR, Herman B, Cascio WE. The pH paradox in ischemia-reperfusion injury to cardiac myocytes. *EXS* 76: 99–114, 1996.
34. Lesnefsky EJ, Moghaddas S, Tandler B, Kerner J, Hoppel CL. Mitochondrial dysfunction in cardiac disease: ischemia—reperfusion, aging, and heart failure. *J Mol Cell Cardiol* 33: 1065–1089, 2001. doi:10.1006/jmcc.2001.1378.
35. Li X, Alvarez B, Casey JR, Reithmeier RA, Fliegel L. Carbonic anhydrase II binds to and enhances activity of the Na<sup>+</sup>/H<sup>+</sup> exchanger. *J Biol Chem* 277: 36085–36091, 2002. doi:10.1074/jbc.M111952200.
36. Li X, Liu Y, Alvarez BV, Casey JR, Fliegel L. A novel carbonic anhydrase II binding site regulates NHE1 activity. *Biochemistry* 45: 2414–2424, 2006. doi:10.1021/bi051132d.
37. Lim HW, New L, Han J, Molkentin JD. Calcineurin enhances MAPK phosphatase-1 expression and p38 MAPK inactivation in cardiac myocytes. *J Biol Chem* 276: 15913–15919, 2001. doi:10.1074/jbc.M100452200.
38. Loiselle FB, Morgan PE, Alvarez BV, Casey JR. Regulation of the human NBC3 Na<sup>+</sup>/HCO<sub>3</sub><sup>-</sup> cotransporter by carbonic anhydrase II and PKA. *Am J Physiol Cell Physiol* 286: C1423–C1433, 2004. doi:10.1152/ajpcell.00382.2003.
39. Moyer JH, Ford RV. Laboratory and clinical observations on ethoxzolamide (cardrase) as a diuretic agent. *Am J Cardiol* 1: 497–504, 1958. doi:10.1016/0002-9149(58)90121-8.
40. Murphy E, Steenbergen C. Mechanisms underlying acute protection from cardiac ischemia-reperfusion injury. *Physiol Rev* 88: 581–609, 2008. doi:10.1152/physrev.00024.2007.
41. Okamura T, Miura T, Takemura G, Fujiwara H, Iwamoto H, Kawamura S, Kimura M, Ikeda Y, Iwatate M, Matsuzaki M. Effect of caspase inhibitors on myocardial infarct size and myocyte DNA fragmentation in the ischemia-reperfused rat heart. *Cardiovasc Res* 45: 642–650, 2000. doi:10.1016/S0008-6363(99)00271-0.
42. Orłowski A, De Giusti VC, Morgan PE, Aiello EA, Alvarez BV. Binding of carbonic anhydrase IX to extracellular loop 4 of the NBCe1 Na<sup>+</sup>/HCO<sub>3</sub><sup>-</sup> cotransporter enhances NBCe1-mediated HCO<sub>3</sub><sup>-</sup> influx in the rat heart. *Am J Physiol Cell Physiol* 303: C69–C80, 2012. doi:10.1152/ajpcell.00431.2011.
43. Panagiotopoulos S, Daly MJ, Nayler WG. Effect of acidosis and alkalosis on postischemic Ca gain in isolated rat heart. *Am J Physiol Heart Circ Physiol* 258: H821–H828, 1990.
44. Pedersen SF, O'Donnell ME, Anderson SE, Cala PM. Physiology and pathophysiology of Na<sup>+</sup>/H<sup>+</sup> exchange and Na<sup>+</sup>-K<sup>+</sup>-2Cl<sup>-</sup> cotransport in the heart, brain, and blood. *Am J Physiol Regul Integr Comp Physiol* 291: R1–R25, 2006. doi:10.1152/ajpregu.00782.2005.
45. Pfeffer MA, Braunwald E. Ventricular remodeling after myocardial infarction. Experimental observations and clinical implications. *Circulation* 81: 1161–1172, 1990. doi:10.1161/01.CIR.81.4.1161.
46. Preckel B, Schlack W, Obal D, Barthel H, Ebel D, Grunert S, Thämer V. Effect of acidotic blood reperfusion on reperfusion injury after coronary artery occlusion in the dog heart. *J Cardiovasc Pharmacol* 31: 179–186, 1998. doi:10.1097/00005344-199802000-00002.
47. Qiao X, Xu J, Yang QJ, Du Y, Lei S, Liu ZH, Liu X, Liu H. Transient acidosis during early reperfusion attenuates myocardium ischemia reperfusion injury via PI3k-Akt-eNOS signaling pathway. *Oxid Med Cell Longev* 2013: 126083, 2013. doi:10.1155/2013/126083.
48. Queliconi BB, Kowaltowski AJ, Gottlieb RA. Bicarbonate increases ischemia-reperfusion damage by inhibiting mitophagy. *PLoS One* 11: e0167678, 2016. doi:10.1371/journal.pone.0167678.
49. Saurin AT, Martin JL, Heads RJ, Foley C, Mockridge JW, Wright MJ, Wang Y, Marber MS. The role of differential activation of p38-mitogen-activated protein kinase in preconditioned ventricular myocytes. *FASEB J* 14: 2237–2246, 2000. doi:10.1096/fj.99-0671.com.
50. Scaduto RC Jr, Grotjohann LW. Measurement of mitochondrial membrane potential using fluorescent rhodamine derivatives. *Biophys J* 76: 469–477, 1999. doi:10.1016/S0006-3495(99)77214-0.
51. Scheibe RJ, Gros G, Parkkila S, Waheed A, Grubb JH, Shah GN, Sly WS, Wetzel P. Expression of membrane-bound carbonic anhydrases IV, IX, and XIV in the mouse heart. *J Histochem Cytochem* 54: 1379–1391, 2006. doi:10.1369/jhc.6A7003.2006.
52. Vandenberg JI, Carter ND, Bethell HW, Nogradi A, Ridderstråle Y, Metcalfe JC, Grace AA. Carbonic anhydrase and cardiac pH regulation. *Am J Physiol Cell Physiol* 271: C1838–C1846, 1996. doi:10.1152/ajpcell.1996.271.6.C1838.
53. Vandenberg JI, Metcalfe JC, Grace AA. Mechanisms of pH<sub>i</sub> recovery after global ischemia in the perfused heart. *Circ Res* 72: 993–1003, 1993. doi:10.1161/01.RES.72.5.993.
54. Vargas LA, Alvarez BV. Carbonic anhydrase XIV in the normal and hypertrophic myocardium. *J Mol Cell Cardiol* 52: 741–752, 2012. doi:10.1016/j.yjmcc.2011.12.008.
55. Vargas LA, Díaz RG, Swenson ER, Pérez NG, Álvarez BV. Inhibition of carbonic anhydrase prevents the Na<sup>+</sup>/H<sup>+</sup> exchanger 1-dependent slow force response to rat myocardial stretch. *Am J Physiol Heart Circ Physiol* 305: H228–H237, 2013. doi:10.1152/ajpheart.00055.2013.
56. Vargas LA, Pinilla OA, Díaz RG, Sepúlveda DE, Swenson ER, Pérez NG, Álvarez BV. Carbonic anhydrase inhibitors reduce cardiac dysfunction after sustained coronary artery ligation in rats. *Cardiovasc Pathol* 25: 468–477, 2016. doi:10.1016/j.carpath.2016.08.003.
57. Vargas LA, Velasquez FC, Alvarez BV. Compensatory role of the NBCn1 sodium/bicarbonate cotransporter on Ca<sup>2+</sup>-induced mitochondrial swelling in hypertrophic hearts. *Basic Res Cardiol* 112: 14, 2017. doi:10.1007/s00395-017-0604-7.

58. **Vaughan-Jones RD, Spitzer KW, Swietach P.** Intracellular pH regulation in heart. *J Mol Cell Cardiol* 46: 318–331, 2009. doi:[10.1016/j.yjmcc.2008.10.024](https://doi.org/10.1016/j.yjmcc.2008.10.024).
59. **Villa-Abrille MC, Cingolani E, Cingolani HE, Alvarez BV.** Silencing of cardiac mitochondrial NHE1 prevents mitochondrial permeability transition pore opening. *Am J Physiol Heart Circ Physiol* 300: H1237–H1251, 2011. doi:[10.1152/ajpheart.00840.2010](https://doi.org/10.1152/ajpheart.00840.2010).
60. **Zheng M, Hou R, Xiao RP.** Acidosis-induced p38 MAPK activation and its implication in regulation of cardiac contractility. *Acta Pharmacol Sin* 25: 1299–1305, 2004.
61. **Zheng M, Reynolds C, Jo SH, Wersto R, Han Q, Xiao RP.** Intracellular acidosis-activated p38 MAPK signaling and its essential role in cardiomyocyte hypoxic injury. *FASEB J* 19: 109–111, 2005. doi:[10.1096/fj.04-2607fje](https://doi.org/10.1096/fj.04-2607fje).

